Hindawi
Advances in Materials Science and Engineering
Volume 2019, Article ID 6487060, 7 pages
https://doi.org/10.1155/2019/6487060

Research Article

The Effect of Microsized Aluminum Powder on Thermal Decomposition of HNIW (CL-20)

Xiaoxiang Mao, Chenguang Zhu, Yanchun Li, Yifan Li, Longfei Jiang, and Xiaoming Wang

Nanjing University of Science and Technology, Xiaolingwei 200, 210094 Nanjing, China

Correspondence should be addressed to Chenguang Zhu; zcg_lnkz@163.com

Received 8 January 2019; Revised 11 March 2019; Accepted 24 March 2019; Published 17 April 2019

Academic Editor: Marinos Pitsikalis

DSC experiments were conducted on the 2,4,6,8,10,12-hexanitro-2,4,6,8,10,12-hexaaza-tetracyclo-[5.5.0.0^{5,9}.0^{3,11}]-dodecane (also known as HNIW or CL-20) and CL-20 containing 10 wt.% microsized aluminum (Al) powders. The kinetic parameters of CL-20 and CL-20/Al were obtained by ASTM685 and Friedman methods, respectively, indicating that Al powder decreases the activation energy of CL-20 slightly and has a catalytic effect on the thermal decomposition of CL-20. By the method of nonlinear multivariate regression, kinetic models of CL-20 and CL-20/Al were derived as $f(\alpha) = (1-\alpha)^n(1 + k_{cat} \cdot \alpha)$, where the $\lg k_{cat}$ of CL-20 and CL-20/Al is 1.97 and 2.12, respectively, showing that the autocatalytic ability of CL-20 had been increased by adding Al powder. From the SEM images of CL-20/Al and the XRD pattern of the decomposition residues of CL-20/Al, it can be inferred that partial combustion of Al particles happened in the microscale view and led to the release of heat.

1. Introduction

Aluminized explosives are made by adding different proportions and particle sizes of aluminum powder to high-energy explosives, aiming to promote significantly the performance of hybrid explosives, such as detonation heat and bubble energy of underwater explosion. Therefore, aluminized explosive has been widely used in military and industrial fields and also become a research hotspot. For a long time, the detonation of aluminized explosives, including the theme of secondary reaction theory, calculation of detonation parameters, and equations of state of detonation products, has been discussed in most of the literatures [1–6]. However, in recent years, there have been more and more studies on the thermal decomposition of aluminized explosives on the perspective of thermal safety.

2,4,6,8,10,12-hexanitro-2,4,6,8,10,12-hexaaza-tetracyclo-[5.5.0.0^{5,9}.0^{3,11}]-dodecane (also known as HNIW or CL-20) is a very high energy density material with potential for widespread applications in munitions [7, 8]. CL-20 displays an interesting behavior during its decomposition as both heating rate and isothermal studies have evidenced an autocatalysis process [9]. The effect of the additives on the thermal behavior of CL-20 also has been studied by scholars, especially the additives such as binder, plasticizer, and desensitizer [10]. In previous studies about thermal decomposition of CL-20 adding of Al powder, somewhat contradictory results were reported. Zhang et al. investigated the effect of Al on polymorphic transition of CL-20 under heat stimulation. They claimed that ε-CL-20 mixed with Al maintained the original form transition characteristics, and there was no distinct effect in the initial temperature of phase transition [11]. But Sun et al. reported that the peak temperature of the crystal transition of ε-CL-20 increased after the addition of nanosized aluminum powders, and the apparent activation energies also increased, indicating that nanosized aluminum exerted an inhibitory effect on the crystal transition of ε-CL-20 [12]. Xiang et al. believed that both of the nanosized (50 nm) and microsized (10 μm) Al powder had the catalytic effect on CL-20, and the activation energy of CL-20 could be decreased very much by microsized Al powder rather than nanosized Al powder since the latter was easy to form an oxide layer [13]. In fact, microsized aluminum powder is generally additive to explosive rather

than nanosized aluminum powder, due to its easy preparation, low price, and stable performance. Therefore, the interaction mechanism between microsized Al powder and CL-20 in the process of thermal decomposition is worth of study, including the participation in reaction, energy release, and heat dissipation of Al.

Our previous study [14] was conducted based on the ignition performance of three kinds of explosives (RDX, HMX, and CL-20) mixed with different mass fractions of Al powders. The results showed that only CL-20 containing 10 wt.% Al powders could release more energy than that of pure CL-20. The main purpose of this paper is to further investigate the effect of microsized Al powders on the thermal decomposition of CL-20 from the following aspects: thermal decomposition kinetics of CL-20 and CL-20/Al by DSC, appearances and particle size of CL-20 and CL-20/Al by SEM, and the decomposition residues analysis of CL-20/Al by XRD.

2. Experimental

2.1. Materials. The CL-20 used in the tests was supplied by Qingyang Chemical Co., Ltd. The Al powder mixed with CL-20 was provided by Tangshan Weihao Magnesium Powder Co., Ltd. The average particle size of CL-20 and Al powder was 80 mesh (124 μm) and 350 mesh (42 μm), respectively. Mixtures of 90 wt.% CL-20 and 10 wt.% Al powder were prepared uniformly.

2.2. Instruments. The differential scanning calorimetry (DSC) tests were carried out by the NETZSCH STA 449 C simultaneous thermal analyzer made in Germany. The images of CL-20 crystals and CL-20/Al were characterized by field-emission scanning electron microscopy (FESEM, JEOL JSM-7800F Prime). XRD (Bruker D8 Advance) was used to characterize the polymorph of experimental residues of CL-20/Al from 5° to 80°.

2.3. Experimental Conditions. Samples of CL-20 and CL-20/Al weight about 1 mg were employed for DSC experiments. The samples were placed in Al_2O_3 pans with laser-drilled pinhole (75 μm) lids. High-purity argon was used to purge the DSC at a rate of 20 mL·min^{-1}. In order to derive kinetic information, samples were heated from ambient temperature to 400°C using heating rates (β) of 1, 2, 4, and 5 K·min^{-1}, respectively. After testing for so many times, we found that, the heating rates should be lower than 7 K·min^{-1}. Because the highly strained molecular cage structure made CL-20 a very high energy density material, if the heating rate is higher than 7 K·min^{-1}, CL-20 is prone to thermal explosion in the DSC test, and the properties of thermal decomposition cannot be obtained. The α-Al_2O_3 was used as the reference sample to correct the reference instrument. The equipment was corrected before each test.

3. Results and Discussion

3.1. DSC Curves of CL-20 and CL-20/Al. The DSC curves shown in Figure 1 illustrate the thermal behavior of CL-20 by heating at 1, 2, 4, and 5 K·min^{-1}, respectively. With the increase of the heating rate, the DSC curves of CL-20 gradually shift to the direction of temperature increase. Based on this characteristic of dynamic DSC experimental result, it could be judged empirically as an autocatalytic reaction [15]. As shown in Table 1, all of the characteristic temperatures including the onset temperature (T_e), peak temperature (T_p), and final temperature (T_f) are delayed, in which the peak temperature of CL-20 increased from 223.4 to 241.4°C. Meanwhile, as the heating rate increases, the exothermic curves become steeper, indicating that thermal decomposition becomes intense. In our experience, the CL-20 is easy to explode if the heating rate is higher than 7 K·min^{-1}.

Figure 2 shows the same trend of CL-20 with 10% Al powders as Figure 1. Considering that the mass fraction of aluminum powder is only 10%, the influence of aluminum powder on the characteristic temperature of explosives is not likely to be significant. However, by comparing the data of characteristic temperatures and exothermic enthalpy (ΔH) as shown in Table 1, some tiny and complex differences can be found. Firstly, the T_p and T_f of CL-20/Al are lower than or equal to that of CL-20 (except T_p at 5 K·min^{-1}), which could be ascribed to the thermal conductivity of the Al powder. However, the exothermic enthalpy (ΔH) measured by DSC is normally inaccurate because the tests were carried out in an open environment, and the purge atmosphere would take part of the heat away. However, the irregular variation trend of ΔH of CL-20/Al could be used for qualitative judgment on the nonideal property of the aluminized explosive. As shown in Table 1, ΔH of CL-20/Al heating at 2 K·min^{-1} or 4 K·min^{-1} was higher than that of CL-20, indicating that part of Al powders participated in reaction and released heat. Whereas, by repetitious experiments, the ΔH of CL-20/Al at 5 K·min^{-1} was the lowest one, indicating that the Al powder not only failed to participate in the reaction but also hindered the complete heat release of CL-20 during thermal decomposition process.

3.2. Calculation of the Kinetic Parameters of Thermal Decomposition. The ASTM698 and Freidman method were used to determine the Arrhenius parameters for the thermal decomposition of CL-20 and CL-20/Al, respectively. The ASTME698 technique occupies an intermediate position between the model fitting and model-free methods. According to the Designation E698-11 [16], the plot lgβ versus $1/T_p$ could be made, where T_p is the corrected peak temperature in K, by calculating and constructing a least squares "best fit" line through these point. The slope of this "best fit" line is taken as the value for $d\lg\beta/d(1/T_p)$, and the activation energy (E) and preexponential factor (A) could be obtained from equations (1) and (2), respectively, where R is the universal gas constant:

$$E = -2.19R\left[\frac{d\lg(\beta)}{d\left(1/T_p\right)}\right], \tag{1}$$

$$A = \frac{\beta E}{RT_p^2}\exp\left(\frac{E}{RT_p}\right). \tag{2}$$

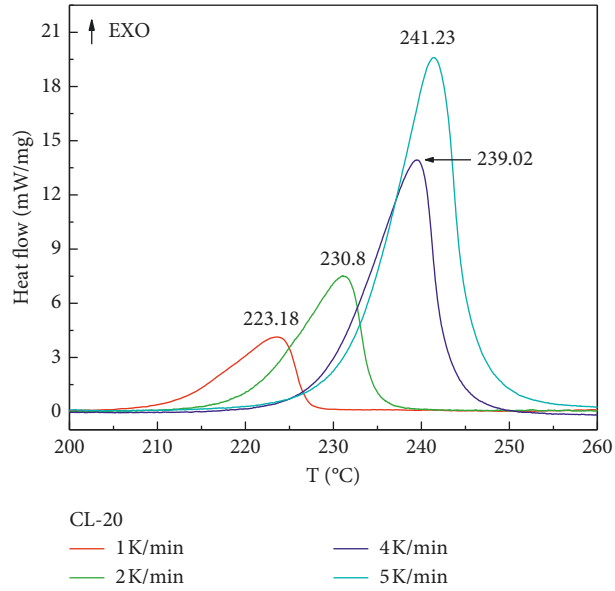

Figure 1: DSC curves of CL-20 under different heating rates (β) of 1, 2, 4, and 5 K·min^{-1}.

Table 1: The characteristic temperatures and exothermic enthalpy of DSC curves for CL-20 and CL-20/Al at different heating rates.

β (K·min^{-1})	T_e (°C)		T_p (°C)		T_f (°C)		ΔH (J·g^{-1})	
	CL-20	CL-20/Al	CL-20	CL-20/Al	CL-20	CL-20/Al	CL-20	CL-20/Al
1	211.5	212.2	223.4	222.5	227.0	226.5	2567	2348
2	220.3	220.3	231.2	230.8	234.6	234.5	2214	2250
4	228.6	228.8	239.5	239.1	243.0	242.5	2153	2287
5	231.7	231.3	241.4	242.0	245.7	245.7	2433	1880

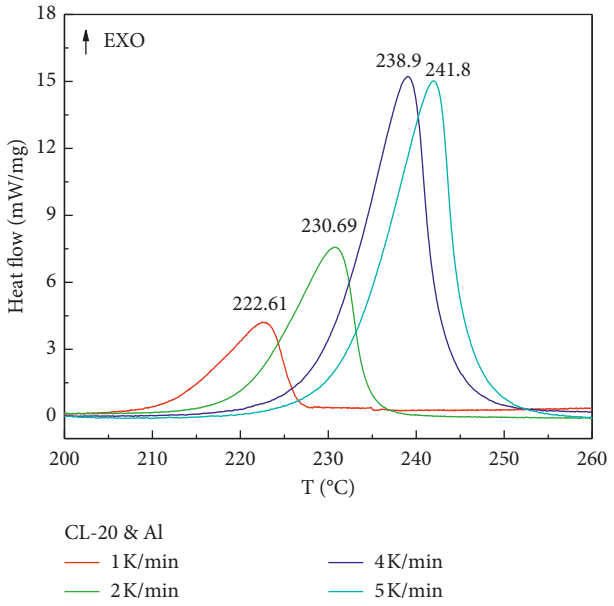

Figure 2: DSC curves of CL-20/Al under different heating rates (β) of 1, 2, 4, and 5 K·min^{-1}.

Figure 3 shows the plots of $\lg(\beta)$ against $1/T_p$ of CL-20 and CL-20/Al, respectively. The activation energy of CL-20 and CL-20/Al obtained from the slope of the plots is 179.18 ± 2.5 kJ·mol^{-1} and 170.37 ± 0.91 kJ·mol^{-1}, respectively. Meanwhile, the values of $\ln(A)$ were also calculated as 16.03 min^{-1} and 15.18 min^{-1}. The results show that adding 10 wt.% microsized Al powder slightly decreases the activation energy of CL-20, indicating that the Al powder may have a catalytic effect on the thermal decomposition of CL-20.

The most common differential isoconversional method is that of Friedman, which was also used to evaluate the model-free kinetics of two samples. Friedman proposed to apply the logarithm of $d\alpha/dt$ as a function of reciprocal temperature at any conversion (α), as shown in the following equation:

$$\frac{d\alpha}{dt} = A_\alpha f(\alpha)\exp\left(-\frac{E_\alpha}{RT}\right),$$
$$\ln\left[\left(\frac{d\alpha}{dt}\right)\right] = \ln\left[A_\alpha f(\alpha)\right] - \frac{E_\alpha}{RT}, \quad (3)$$

where $f(\alpha)$ is the reaction mechanism function in differential form and a constant at any fixed value of conversion. The dependence of $\ln(d\alpha/dt)$ on $1/T$ shows a straight line with the slope equal to $-E_\alpha/R$ and the intercept equal to $\ln[A_\alpha f(\alpha)]$. Therefore, linear fitting was performed to estimate the effective E_α for the set of different conversions. For complex multistage reactions, this method gives the effective E_α which depends on the extent of conversion.

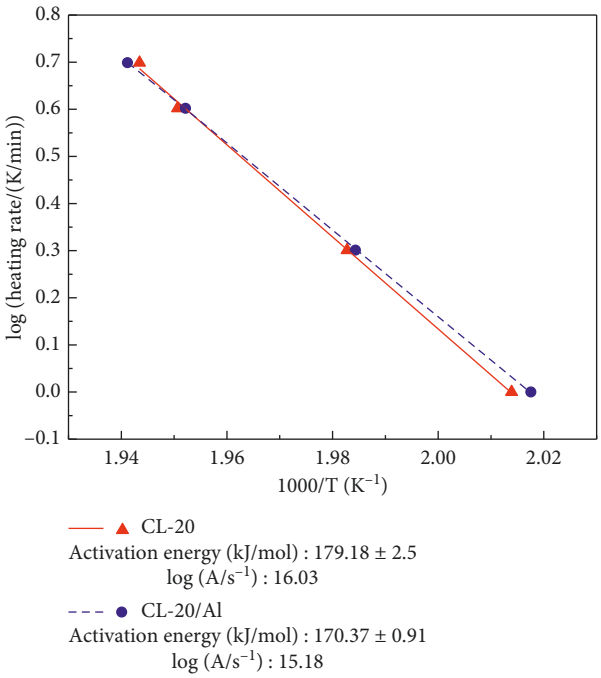

Figure 3: ASTM698 fitting plots for thermal decomposition of CL-20 and CL-20/Al at four heating rates.

Furthermore, for single-stage reaction with known function $f(\alpha)$, the preexponential factor (A_α) can be calculated [17]. The calculation results by Friedman are tabulated in Table 2. The variation trend of E_α with different α is shown in Figure 4.

As described above, the apparent activation energy calculated by Friedman method is not a constant, but a value varies with the conversion. At each given α, the value of E_α is determined from the slope of a plot of $\ln(d\alpha/dt)$ against $1/T$ [18]. As shown in Table 2 and Figure 4, the variation of activation energy (E_α) is relatively stable as α varies from 0.1 to 0.7. The average values of E_α $(\alpha = 0.1 - 0.7)$ of CL-20 and CL-20/Al are 173.45 kJ·mol^{-1} and 169.53 kJ·mol^{-1}, respectively, indicating that the Al powder decreases the activation energy of CL-20 a little. This result is consistent with the result calculated by ASTM698. It has further confirmed that the Al powder has a catalytic effect on the thermal decomposition of CL-20, especially during the early stage of thermal decomposition.

3.3. Determination of the Kinetic Model by the Method of Nonlinear Multivariate Regression. Thermal decomposition of energetic materials is a kind of reaction happening in the solid heterogeneous system. The reaction model of energetic materials is usually not completed in one step, but in a multistep reaction process. The relationship between each step is complicated. The corresponding dynamic model functions of each step may be different. Therefore, traditional methods cannot accurately describe the kinetic model of such a complex system. For example, Singh et al. proved that the traditional model-fitting methods cannot describe the complex process of thermal composition of RDX [19]. The nonlinear multivariate regression is an indispensable method to derive kinetic models. This technique is the only way to decide between different reaction models and get a global model which gives reliable results for the whole parameter range.

As shown in Figures 5 and 6, the kinetic model simulated by software (NETZSCH Thermo kinetics) fits the experimental data very well, and the optimum values of kinetic parameters are listed in Table 3. The values of correlation coefficient are 0.994 (CL-20) and 0.993 (CL-20/Al), respectively. According to the fitting results, the kinetic model for both CL-20 and CL-20/Al is $f(\alpha) = (1-\alpha)^n (1 + k_{cat} \cdot \alpha)$, where n is the reaction order and k_{cat} is the autocatalytic kinetic rate constant. Both the reaction order of CL-20 and CL-20/Al is 1, and $\lg k_{cat}$ of two samples is 1.97 and 2.12, respectively, showing that the CL-20/Al autocatalytic ability is higher than that of CL-20. It also can be seen that the optimum value of CL-20/Al activation energy (160.13 kJ·mol^{-1}) is also lower than that of CL-20 (175.9 kJ·mol^{-1}), confirming the conclusions from ASTM698 and Friedman methods that the Al powder has a catalytic effect on the thermal decomposition of CL-20.

3.4. Analysis of Reaction Mechanism of CL-20/Al by SEM and XRD. Our previous study shows that Al not only cannot participate in the reaction or combustion but also hinders complete reaction of RDX and HMX during the thermal decomposition. However, only CL-20 containing 10 wt.% Al powder can release more energy than that of pure CL-20 in some cases [12]. Therefore, it is worth to investigate why Al only can react with CL-20 and the reaction mechanism of CL-20/Al, while the melting point of Al (660°C) is obviously higher than thermal decomposition temperature of CL-20 (236°C). Based on the analysis of thermal kinetics, we decided to investigate the microstructure and characterization of the CL-20/Al by SEM and XRD.

It can be seen clearly from Figure 7(a) that the crystal quality of raw CL-20 particles is high with little crystal defects, and the shapes are mostly short diamond rods with blunt edge. As shown in Figures 7(b) and 7(c), the Al particle is much smaller than CL-20 and adsorbed on the surface of explosive particles similar to the agglomeration phenomenon. That is to say there are many aggregated particles consisting of Al particles wrapped around CL-20 particles in the microscale view. Therefore, such situation could be imaged and speculated that, as the CL-20 particle is ignited and releases heat, the temperature around the CL-20 particles rises rapidly and is possibly close to the melting point of Al, leading to the partial combustion of Al particles.

Figure 8 shows XRD patterns of the residues of the DSC test for CL-20/Al which has been heated from ambient temperature to 400°C. Although most of the diffraction peaks with low intensity are too weak and hidden in the noise, a very clear diffraction peaks at 38.2° could be seen and assigned to hexagonal aluminum nitride (JCPDS No. 00-003-1144), indicating the existence of aluminum nitride (AlN) particles in the residues. In addition, the peak located at 6° can be indexed to the (002) planes of the orthorhombic

Table 2: Activation energy (E_α) and preexponential factor (ln A_a) of CL-20 and CL-20/Al calculated by Friedman method.

Conversion (α)	CL-20			CL-20/Al		
	E_α (kJ·mol^{-1})	Deviation	ln A_α (s^{-1})	E_α (kJ·mol^{-1})	Deviation	ln A_α (s^{-1})
0.1	178.21	±2.25	15.73	162.22	±3.16	14.12
0.2	177.4	±0.6	15.88	165.9	±1	14.73
0.3	179.37	±1.32	16.22	170.1	±1.59	15.3
0.4	179.73	±1.9	16.35	171.99	±2.58	15.6
0.5	176.23	±2.41	16.08	172.3	±3.04	15.73
0.6	168.49	±3.88	15.36	172.46	±3.57	15.85
0.7	154.73	±6.1	14.02	171.75	±4.06	15.88
0.8	129.35	±7.34	11.46	157.9	±10.03	14.54
0.9	87.02	±18.62	7.06	109.16	±25.84	9.47
Average (0.1–0.7)	173.45		15.66	169.53		15.31

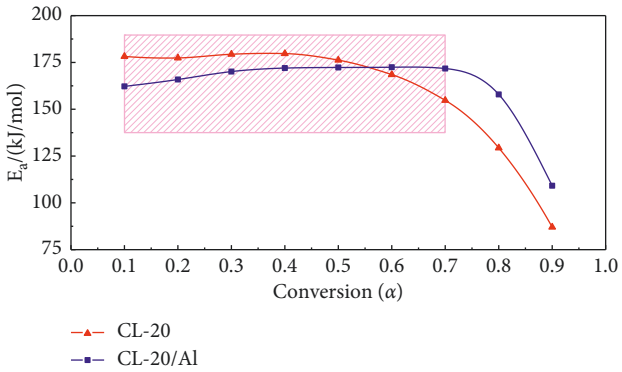

Figure 4: The variation of activation energy (E_α) of CL-20 and CL-20/Al depend on conversion ($\alpha = 0.1 - 0.9$, with 0.1 increment) calculated by Friedman method.

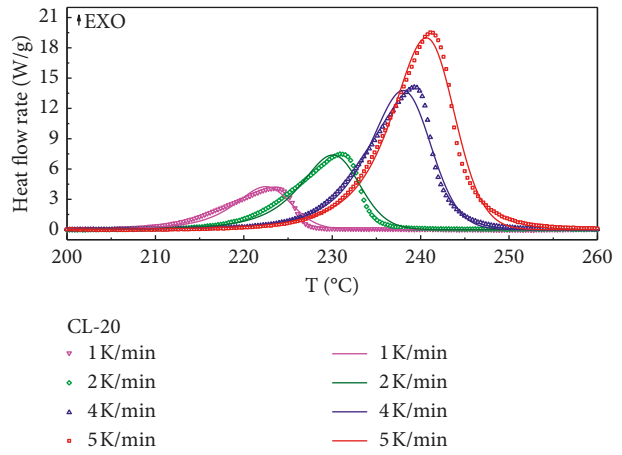

Figure 5: Comparison between experiments and simulation of DSC curves for CL-20 heating at 1 K·min^{-1}, 2 K·min^{-1}, 4 K·min^{-1}, and 5 K·min^{-1}.

carbon (JCPDS No. 01-074-2330), indicating the existence of C in the residues. Since the DSC experiments were carried out in the argon atmosphere, there is no nitrogen atmosphere. It is confirmed that the nitrogen element of AlN is provided from products of CL-20 thermal decomposition. Thus, it can be inferred that Al reacts with CL-20 decomposition products in some way and produce AlN.

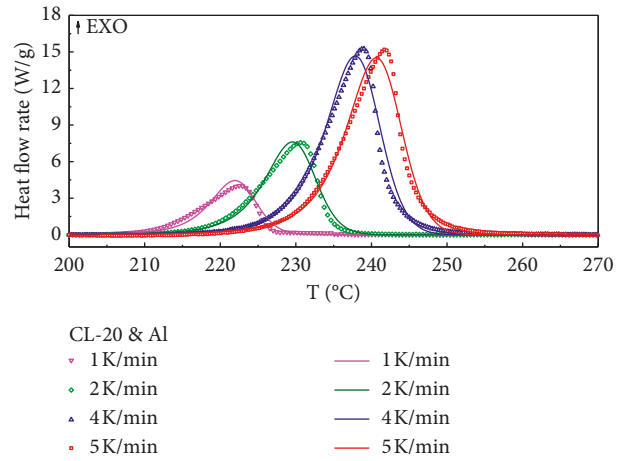

Figure 6: Comparison between experiments and simulation of DSC curves for CL-20/Al heating at 1 K·min^{-1}, 2 K·min^{-1}, 4 K·min^{-1}, and 5 K·min^{-1}.

Table 3: Optimum values of kinetic parameters of CL-20 and CL-20/Al by the method of nonlinear multivariate regression.

kinetic parameters	CL-20	CL-20/Al
lg A (s^{-1})	14.45	12.74
E_α (kJ·mol^{-1})	175.90	160.13
Reaction order (n)	1	1
lgk_{cat}	1.97	2.12
Correlation coefficient	0.994	0.993

In the view of microscale of the thermal decomposition tests, we believe that the explosion heat and enthalpy of formation are reasonable to explain mentioned question. Explosion heat is the heat released instantaneously during the explosion and almost unaffected by the time. It is known that the explosion heat of CL-20 is 6.08 MJ·kg^{-1}, much more than that of RDX (5.29 MJ·kg^{-1}) and HMX (5.25 MJ·kg^{-1}) [19], and as long as the explosive explode, part of the heat is released instantaneously. Moreover, the enthalpy of formation of RDX is 279 kJ·kg^{-1}, HMX is 253 kJ·kg^{-1}, and CL-20 is 1006 kJ·kg^{-1} [20]. Therefore, we speculate that because the explosion heat and enthalpy of formation of CL-20 is far higher than that of RDX and HMX, which can be considered as a higher ability of instantaneous heat release, high-

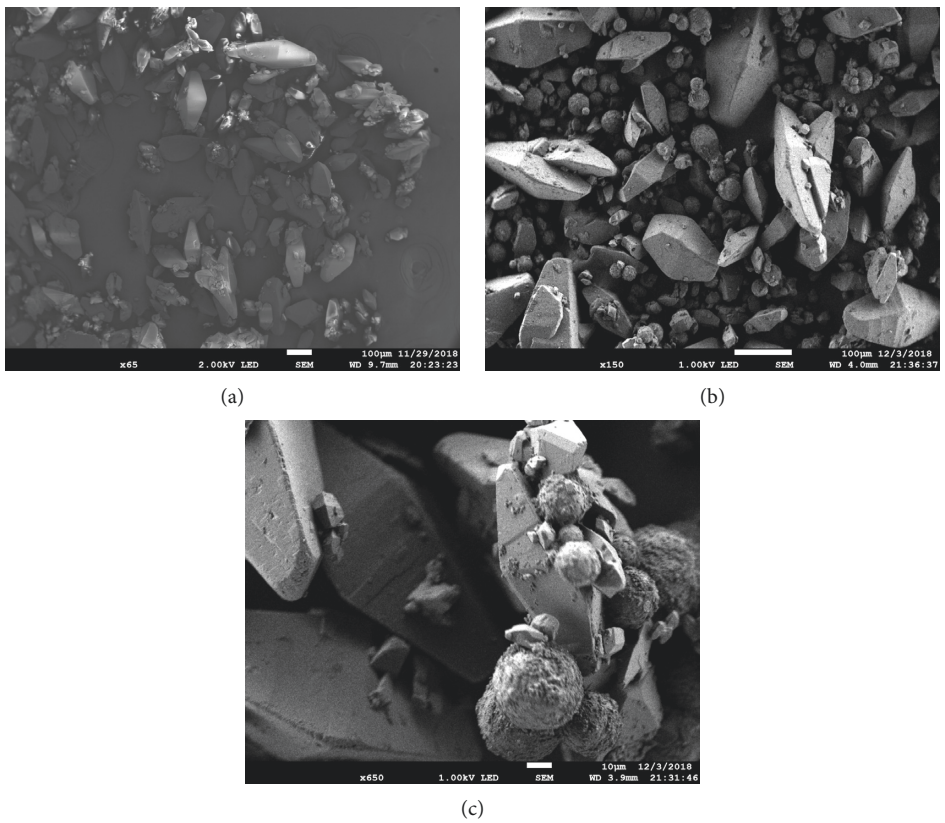

(a) (b)

(c)

Figure 7: SEM images of (a) CL-20, (b) CL-20/Al, and (c) magnified CL-20/Al.

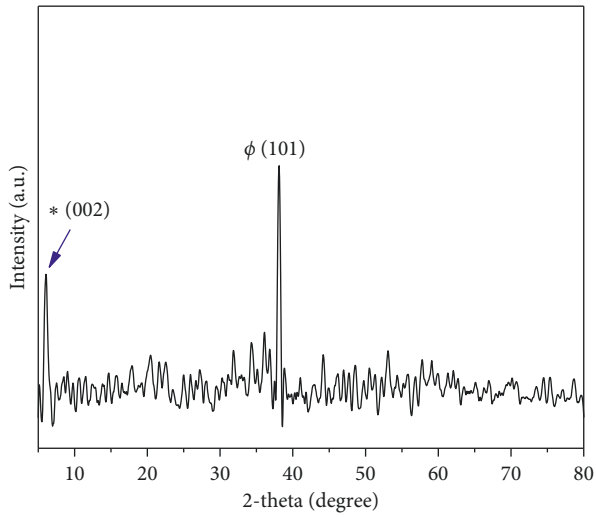

Figure 8: XRD pattern of experimental residues of CL-20/Al.

temperature zone at microscale may be formed with CL-20 particles as the core. In other words, the temperature at which the Al particles participate in the reaction may be reached by the heat instantaneously released from CL-20; thus, the partial combustion of the Al powder can be promoted. It is generally known that hotspot initiation theory described an early stage of initiation mechanism of explosives. Correspondingly, we assume that, in the micron scale view of CL-20/Al composite, high-temperature zones of the agglomeration structure can be formed, which can promote the partial combustion of the Al powder in the thermal decomposition of CL-20. In such high-temperature zones, a relative ideal and self-sustained reaction could happen.

4. Conclusions

Comparable kinetic parameters of CL-20 and CL-20/Al were obtained by various methods, indicating that the Al powder decreases the activation energy of CL-20 slightly. Overall, it demonstrates that the Al powder has a catalytic effect on the thermal decomposition of CL-20, especially during the early stage of the thermal decomposition process. By the method of nonlinear multivariate regression, we know the thermal decomposition of CL-20 and CL-20/Al belongs to autocatalytic behavior, which is consistent with the findings reported by Turcotte et al. [9]. The kinetic model of CL-20 and CL-20/Al is derived as $f(\alpha) = (1-\alpha)^n(1 + k_{cat} \cdot \alpha)$, where $\lg k_{cat}$ of CL-20 and CL-20/Al is 1.97 and 2.12, showing that CL-20/Al has higher autocatalytic ability than CL-20. From the SEM images of CL-20/Al and the XRD pattern of the CL-20/Al thermal decomposition residues, it is inferred that, in the microscale view, partial combustion of Al particles happens and led to heat release because of the agglomeration structure of the CL-20/Al mixture. We speculate that, since CL-20 has a higher ability of

instantaneous heat release, a localized high-temperature region could be formed in the mixture of CL-20/Al at microscale. As the surface reaction temperature of Al particles reached, Al begins to participate in the reaction.

Data Availability

The DSC and XRD data used to support the findings of this study are included within the article. Previously reported (Explosion Heat and Enthalpy of Formation) data were used to support this study and are available at ISBN 978-7-5682-2558-8. These prior studies (and datasets) are cited at relevant places within the text as references [16].

Conflicts of Interest

The authors declare that they have no conflicts of interest.

Acknowledgments

This work was supported by the National Science Foundation of China under Grant nos. 51676100 and 51076066.

References

[1] H. X. Xu, X. W. Li, F. Q. Zhao et al., "Review on application of nano-metal powders in explosive and propellants," *Chinese Journal of Energetic Materials*, vol. 19, pp. 232–239, 2011.

[2] L. Chen and X. P. Long, *Detonation of Aluminized Explosive*, National Defense Industry Press, Beijing, China, 2004.

[3] M. H. Keshavarz, "Prediction of detonation performance of CHNO and CHNOAl explosives through molecular structure," *Journal of Hazardous Materials*, vol. 166, no. 2-3, pp. 1296–1301, 2009.

[4] B. Patrick, E. D. Helen, D. C. Matthew et al., "Detonation properties of explosives containing nanometric aluminum powder," in *Proceedings of the 12th International Detonation Symposium*, Diego, CA, USA, August 2002.

[5] J. H. Peng, W. H. Chen, H. Su et al., "The effect of aluminum powder upon aluminized explosive underwater detonation performance," *Journal of Safety and Environment*, vol. 4, pp. 177–179, 2004.

[6] D. Liu, L. Chen, C. Wang, and J. Wu, "Aluminum acceleration and reaction characteristics for aluminized CL-20-based mixed explosives," *Propellants, Explosives, Pyrotechnics*, vol. 43, no. 6, pp. 543–551, 2018.

[7] R. L. Simpson, P. A. Urtiev, D. L. Ornellas et al., "CL-20 performance exceeds that of HMX and its sensitivity is moderate," *Propellants, Explosives, Pyrotechnics*, vol. 22, no. 5, pp. 249–255, 1997.

[8] N. B. Bolotina, M. J. Hardie, R. L. Speer, and A. A. Pinkerton, "Energetic materials: variable-temperature crystal structures of γ- and ε-HNIW polymorphs," *Journal of Applied Crystallography*, vol. 37, no. 5, pp. 808–814, 2004.

[9] R. Turcotte, M. Vachon, Q. S. M. Kwok, R. Wang, and D. E. G. Jones, "Thermal study of HNIW (CL-20)," *Thermochimica Acta*, vol. 433, no. 1-2, pp. 105–115, 2005.

[10] H. Zou, S. Chen, X. Li et al., "Thermal behavior and decomposition kinetics of CL-20-based plastic-bonded explosives," *Journal of Thermal Analysis and Calorimetry*, vol. 128, no. 3, pp. 1867–1873, 2017.

[11] P. Zhang, J. Xu, X. Guo et al., "Effect of addictives on polymorphic transition of e-CL-20 in castable systems," *Journal of Thermal Analysis and Calorimetry*, vol. 117, no. 2, pp. 1001–1008, 2014.

[12] L. Sun, S. Yan, and Q. Jiao, "Effects of nano-combustible fuels on ε-CL-20 crystal transition," *Acta Armamentar*, vol. 6, p. 221, 2017.

[13] M. Xiang, Q. Jiao, Y. Zhu, J. Yu, and L. Chen, "Thermal study of HNIW (CL-20) and mixtures containing aluminum powder," *Journal of Thermal Analysis and Calorimetry*, vol. 116, no. 3, pp. 1159–1163, 2014.

[14] X. X. Mao, L. F. Jiang, C. G. Zhu, and X. Wang, "Effects of aluminum powder on ignition performance of RDX, HMX and CL-20 explosives," *Advances in Materials Science and Engineering*, vol. 2018, Article ID 5913216, 8 pages, 2018.

[15] L. Bou-Diab and H. Fierz, "Identification of autocatalytic decomposition by differential scanning calorimety," *Loss Prevention and Safety Promotion in the Process Industries*, in *Proceeding of the 10th International Symposium*, Stockholm, Sweden, June 2001.

[16] ASTM International E698-16, *Standard Test Method for Kinetic Parameters for Thermally Unstable Materials Using Differential Scanning Calorimetry and the Flynn/Wall/Ozawa Method*, ASTM International, West Conshohocken, PA, USA, 2016.

[17] S. Y. Wang, A. A. Kossoy, Y. D. Yao, L. P. Chen, and W. H. Chen, "Kinetics-based simulation approach to evaluate thermal hazards of benzaldehyde oxime by DSC tests," *Thermochimica Acta*, vol. 655, pp. 319–325, 2017.

[18] S. Vyazovkin, A. K. Burnham, and J. M. Criado, "ICTAC kinetics committee recommendations for performing kinetic computations on thermal analysis data," *Thermochimica Acta*, vol. 520, no. 1-2, pp. 1–19, 2011.

[19] G. Singh, S. P. Felix, and P. Soni, "Studies on energetic compounds: Part 31. Thermolysis and kinetics of RDX and some of its plastic bonded explosives," *Thermochimica Acta*, vol. 426, no. 1-2, pp. 131–139, 2005.

[20] X. Y. Ou, *Explosives*, Beijing Institute of Technology Press, Beijing, China, 2014.